# An Energy-Maximising Linear Time Invariant Controller (LiTe-Con) for Wave Energy Devices

Demián García-Violini ⓘ, Yerai Peña-Sanchez ⓘ, Nicolás Faedo ⓘ, and John V. Ringwood ⓘ, *Senior Member, IEEE*

*Abstract*—A Linear Time Invariant (LTI) energy-maximising control strategy for Wave Energy Converters (WECs) is proposed in this paper. Using the fundamental requirement of impedance-matching, the controller is tuned to maximise the energy obtained under polychromatic wave excitation. Given the LTI nature of the proposed controller, the design and implementation procedure is significantly simpler than well-established energy-maximising controllers, including state-of-the-art numerical optimisation routines, which are predominant in this field. Additionally, a LTI constraint handling mechanism is provided. The effectiveness of both the LTI control strategy and the constraint handling mechanism are assessed using regular and irregular waves in unconstrained and constrained cases. The resulting performance is compared to those obtained using existing WEC optimal control strategies. Finally, the benefits, in terms of power production, for both the controller and the constraint handling mechanism are explicitly highlighted by means of an application case.

*Index Terms*—Wave energy, optimal control, impedance-matching, linear time invariant (LTI).

## I. INTRODUCTION

ENERGY AVAILABLE in ocean waves represents an abundant resource which can substantially contribute to the development of new power production strategies. However the commercial viability of wave power production systems is still far from being economically competitive [1]. To reduce the cost of generating energy from ocean waves, control systems are considered as key drivers to maximise energy capture in wave energy systems [2]. In recent years there has been active research into developing control methods and strategies applied to wave energy converters (WECs). In general, WEC optimal control strategies verify the fundamental requirement of impedance-matching, which provides optimal conditions, in the frequency domain, for energy maximising controllers, as well as the maximum reachable absorbed energy [3], [4]. However, as reported in the literature, impedance-matching control strategies are practically not feasible due to their intrinsic non-causality [1], [4]. Additionally, physical constraints (amplitudes, forces, etc) are, in general, not taken into account by available impedance-matching control strategies [5].

With the aim of improving energy capture mechanisms in WECs, a number of control methods and strategies have been reported in the literature (with early studies emerging in the '70 s), such as impedance-matching-based control [6], resistive/reactive control [3], latching control [7], Model Predictive Control (MPC) [8], optimal reference tracking control [9], moment-matching-based (MM-based) control [10], and Spectral/Pseudospectral-based (Sp/Ps-based) control methods [11]. On one hand, the impedance-matching-based control presented in [6] can only deal with monochromatic (regular) waves. On the other hand, using resistive/reactive control strategies, which are commonly considered mainly because these controllers do not require wave excitation force estimation and forecasting, only narrow-band energy absorption can be achieved. Additionally, these strategies do not inherently incorporate constraint handling techniques, and the controller parameters are usually tuned using exhaustive search processes [12]. Regarding the strategies based on latching mechanisms, even though, in theory, they allow for the absorption of significant amount of energy, their implementability and performance have been challenged due to overloads on the latching mechanism [13], the relatively low performance in the case of self-reacting mechanism point-absorbers [14], and the long prediction horizon required for the real-time optimisation in polychromatic (irregular) waves to converge [15]. However, optimisation-based strategies, such as MPC-based, MM-based, or Sp/Ps-based, can deal with physical constraints obtaining (theoretically) optimal solutions [8], [16]. Nevertheless, the implementation of such techniques requires the solution of a constrained optimisation problem at each iteration, which can require a large computation effort and, depending on the computer architecture and the system model complexity, is not always implementable in practice [16]. Additionally, the family of real-time optimisation-based controllers, e.g MPC, MM/Sp/Ps-based control, requires prediction of the excitation force, which, although possible for a given time period, introduces additional uncertainty in the optimisation problem and, consequently, results in performance degradation [17]. Finally,

D. García-Violini is with the Department Science and Technology, National University of Quilmes, Bernal, Argentina (e-mail: demian.garciaviolini@mu.ie).

Y. Peña-Sanchez, N. Faedo, and J. V. Ringwood are with the Department of Electronic Engineering, National University of Ireland Maynooth, W23 F2K8 Maynooth, Ireland (e-mail: yerai.pena.2017@mumail.ie; nicolas.faedo.2017@mumail.ie; john.ringwood@eeng.nuim.ie).

the controller proposed in [9], known as the Simple and Effective (SaE) controller, assumes that the excitation force can be considered as a narrow banded process, then, using an Extended Kalman Filter (EKF), the excitation force amplitude and frequency, are computed. An optimal velocity profile is obtained with an open loop feedforward (FF) structure, which is used as the reference in a traditional reference tracking linear time invariant (LTI) feedback (FB) loop. This FB controller guarantees an interpolation condition using the Internal Model Principle (IMP), for a particular given frequency, generally defined by the particular sea state's peak period. The design and implementation simplicity of this controller is worth highlighting. However, given the challenge involved in the EKF tuning and its sensitivity to design parameters [18], the EKF inclusion directly impacts negatively on the resulting performance. In addition, the performance degradation due to the use of estimators (or forecasters), has a significant effect on the final energy maximising control performance, which is potentially emphasised in non-linear unknown input strategies, where (local) stability assumptions are often violated [17]. Please refer to [16] and [19] for further WEC energy maximising control strategies.

With the same essence of simplicity and efficiency of the SaE controller proposed in [9], this paper proposes an alternative energy maximising controller for WEC systems, in which the design and implementation procedure are significantly simpler than optimisation-based controllers. Based on the impedance-matching principle, using state-of-the-art system identification algorithms, the proposed LTI (LiTe-Con) controller is tuned to approximate the frequency domain energy maximising optimal condition, obtaining a stable and casual LTI controller. In addition, a suboptimal constraint handling mechanism is provided in this study. Furthermore, even though the proposed control strategy essentially provides a broadband energy maximising control method, a trade-off between the target bandwidth and the resulting performance is shown. On the other hand, and unlike the SaE controller [9], in which the instantaneous excitation force, amplitude, and frequency estimations are required to compute an optimal control input, only an excitation force estimate is required for the LiTe-Con controller. Additionally, since the LiTe-Con controller is a causal LTI system, excitation force prediction is not required to compute the energy maximising control force. The complete control structure stability (system, excitation force estimator, and controller) is guaranteed under the separability principle. As mentioned before, the LTI controller strategy proposed in this study is essentially aligned with that proposed in [9]. However, the LiTe-Con results in a simpler controller, in terms of design and implementation as well as, being more efficient in terms of the resulting power production (see Section IV). From a general perspective, as an immediate consequence of only considering LTI systems, it can be mentioned that, in comparison with the SaE controller, the robustness and performance in terms of power production, and implementation of the controller in physical platforms, (e.g. microcontrollers, programmable logic controllers, personal computers, etc), are significantly improved by the LiTe-Con controller, while providing a broadband energy maximising solution. In addition, the LiTe-Con controller can indistinctly
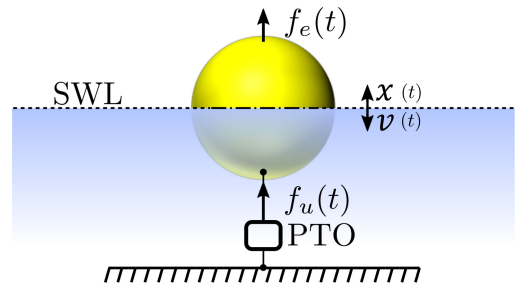


Fig. 1. A single-body floating system, oscillating in heave, is schematically depicted. The lower side of the power take-off is anchored to the sea bed, which provides an absolute reference for device motion. Still water level is denoted by the acronym SWL. The position and velocity of the device are denoted by $x(t)$ and $v(t)$, respectively.

deal with narrow-banded or broad-banded sea states. Within this context, the LiTe-Con controller can be considered (to the best of the authors knowledge) the unique broadband energy maximising controller exclusively based on LTI systems in the wave energy field [1].

The remainder of this paper is organised as follows. Section II articulates standard WEC modelling paradigms and assumptions. The main core of the controller proposed in this study is contained in Section III, in which the impedance-matching basics are recalled, differences between feedback (FB) and feedforward (FF) structures are presented, and the LTI controller and its constraint handling mechanism are introduced. In Section IV, using regular and irregular waves in the unconstrained and constrained cases, the proposed controller performance is assessed with an application case, comparing the results with those obtained using existing controllers in the literature [9], [10]. Finally, conclusions on the overall application of the proposed controller are provided in Section V.

### A. Notation

$Z(\omega)$, $z(t)$ denotes a Fourier transform pair. $Z^{\star}(\omega)$ denotes the complex conjugate of $Z(\omega)$. $\mathbb{Re}\{\cdot\}$ and $\mathbb{Im}\{\cdot\}$ denote the *real-part* and *imaginary-part* operators.

## II. WAVE ENERGY CONVERTER MODEL

In this section, the basics of WEC dynamics and its equations are recalled. Given the nature of the LTI control strategy proposed in this study, the WEC dynamics are represented in the frequency domain. Please refer to [3] for a detailed derivation, or a time domain description, of the equations presented in this section.

As schematically depicted in Fig. 1, a single-body floating WEC system, oscillating in heave, is considered. The useful absorbed energy is extracted from the relative displacement with an absolute reference for device motion, usually the sea bottom, through the Power Take-Off (PTO) system. The external forces acting on the WEC are the excitation from the waves and the control force produced by the PTO. Considering that the WEC device is referenced from its equilibrium position (still water level) in an undisturbed wave field and immersed in an infinite-depth sea, the system is subject to fluid-structure interactions

which are typically modelled using potential flow theory. The fluid is assumed to be inviscid and incompressible, and the flow is considered irrotational.[1] Thus, the model can be expressed in the frequency domain, as follows [3]:

$$\jmath\omega M V(\omega) + Z_r(\omega)V(\omega) + \frac{K_h}{\jmath\omega}V(\omega) = F_{ex}(\omega) + F_u(\omega), \tag{1}$$

where $M$ represents the WEC mass, $V(\omega)$ the WEC heaving velocity, while $F_{ex}(\omega)$ and $F_u(\omega)$ are the wave excitation and PTO forces, respectively. The hydrostatic restoring, or buoyancy, force is related to the device displacement from its equilibrium position and is modelled by a linear term involving the stiffness coefficient $K_h$. The radiation force, depicted in Eq. (1) via the radiation impedance $Z_r(\omega)$, can be generally decomposed as:

$$Z_r(\omega) = B_r(\omega) + \jmath\omega\left(M_a(\omega) + M_\infty\right) = H_r(\omega) + \jmath\omega M_\infty, \tag{2}$$

where $B_r(\omega)$ is the radiation damping (real and even), and $M_a(\omega) + M_\infty$ the radiation reactance, with $M_a(\omega) = A_r(\omega) - M_\infty$, where $A_r(\omega)$ is the added mass and $M_\infty$ the added mass at infinite frequency, i.e. $M_\infty = \lim_{\omega\to\infty} A_r(\omega)$. Additionally, in Eq. (2), $H_r(\omega) = B_r(\omega) + \jmath\omega M_a(\omega)$.

Then, the model expressed in Eq. (1) can be rewritten as:

$$V(\omega) = \frac{1}{Z_i(\omega)}\left[F_{ex}(\omega) + F_u(\omega)\right], \tag{3}$$

where

$$Z_i(\omega) = B_r(\omega) + \jmath\omega\left(M + A_r(\omega) - \frac{K_h}{\omega^2}\right), \tag{4}$$

in which $Z_i(\omega)$ denotes the intrinsic impedance of the floating system. Considering the force-to-velocity mapping in the Laplace domain, get:

$$G(s) = \left.\frac{s}{s^2(M + M_\infty) + s\hat{H}_r(s) + K_h}\right|_{s=\jmath\omega} = \frac{1}{Z_i(\omega)}, \tag{5}$$

where, since $H_r(\omega)$ is commonly computed using boundary-element methods, such as WAMIT [23] or NEMOH [24], $\hat{H}_r(s)$ represents a LTI approximation of $H_r(\omega)$, for $s = \jmath\omega$.

## III. CONTROLLER

This section outlines the proposed causal LiTe-Con control strategy for WECs. To this end, Section III-A recalls the basics of impedance-matching energy maximising control. Then, the LiTe-Con design procedure is described in Sections III-B. Finally, in Section III-C, the constraint handling mechanism is introduced.

### A. Optimal Control Condition

As usual in wave energy control problems [3], the useful absorbed energy, over the time interval $[0, T]$ with $T > 0$, can
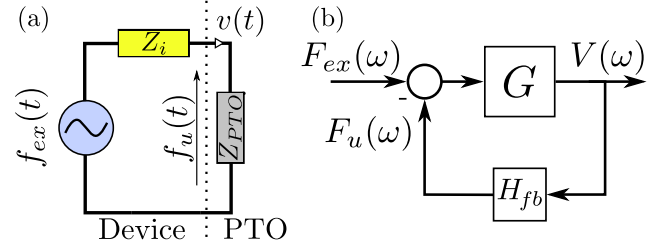
Fig. 2. (a) Impedance-matching problem in WECs represented with its electrical equivalent. (b) Impedance-matching-based controller structure.

be calculated as the integral of converted power

$$E = -\int_0^T v(t)f_u(t)dt. \tag{6}$$

Under the assumptions considered in Section II for Eq. (1), the impedance-matching problem represented in Fig. 2(a), allows the derivation of an optimal condition, in terms of the PTO force $f_u(t)$, for maximum absorbed energy $E$ in Eq. (6), in the frequency domain:

$$F_u(\omega) = -Z_i^\star(\omega)V(\omega). \tag{7}$$

The expression in Eq. (7) has some fundamental issues which are worth highlighting: (a) due to the non-causality of the expression in Eq. (7), a real-time implementation is not possible; (b) the frequency dependency implies a different optimal impedance for each $\omega$; (c) both positive and negative forces (i.e. a bi-directional actuator) are required to achieve the optimal energy absorption condition; and (d) the optimal control law in Eq. (7) does not take into account physical constraints in the WEC/PTO.

The optimal condition, defined in Eq. (7), can be alternatively expressed in terms of an optimal velocity profile $V^{opt}(\omega)$ as:

$$V^{opt}(\omega) = \frac{1}{Z_i(\omega) + Z_i^\star(\omega)}F_{ex}(\omega) = \frac{1}{2B_r(\omega)}F_{ex}(\omega). \tag{8}$$

Note that, when Eq. (7) is satisfied, Eq. (8) defines a purely real frequency dependent mapping, which implies a zero-phase shift between $F_{ex}(\omega)$ and $V^{opt}(\omega)$. Equations (7) and (8) essentially lead to the fundamental WEC control structure depicted in Fig. 2(b) [25], in which, according to Eq. (7), ideally:

$$H_{fb}(\omega) = Z_i^\star(\omega). \tag{9}$$

The expression in Eq. (9) is presented in the literature as the impedance-matching solution to WEC control problems [3]; however, the intrinsic non-causality of $H_{fb}(\omega)$ does not allow for practical implementation of the controller. Additionally, from a sensitivity/robustness perspective, the applicability of the controller in Eq. (9) has been questioned in [5]. To deal with these intrinsic limitations, a monochromatic approach is proposed in [6]. Based on the impedance-matching problem, in Section III-B the problem is restated into a feedforward structure, to approach a broadband control solution.

### B. LTI Control

Considering the impedance-matching control structure presented in Section III-A, both the system $G(s)$ and the controller
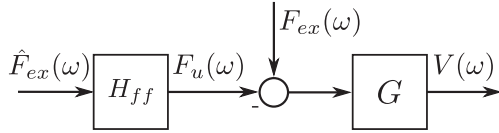
Fig. 3.    Feedforward impedance-matching-based control structure.

$H_{fb}(s)$ can be described in the frequency-domain using the real and imaginary part operators:

$$G(s)\Big|_{s=\jmath\omega} = \mathbb{R}\mathrm{e}\{G(\jmath\omega)\} + \jmath\mathbb{I}\mathrm{m}\{G(\jmath\omega)\}, \qquad (10)$$

$$H_{fb}(s)\Big|_{s=\jmath\omega} = \frac{1}{\mathbb{R}\mathrm{e}\{G(\jmath\omega)\} - \jmath\mathbb{I}\mathrm{m}\{G(\jmath\omega)\}}. \qquad (11)$$

For the sake of simplicity of notation, let $\mathbb{R}\mathrm{e}(G) = \mathbb{R}\mathrm{e}\{G(\jmath\omega)\}$ and $\mathbb{I}\mathrm{m}(G) = \mathbb{I}\mathrm{m}\{G(\jmath\omega)\}$. Then, the optimal mapping from $F_{ex}(\omega)$ to $V^{opt}(\omega)$, described in Eq. (8), can be equivalently expressed as:

$$T^{opt}_{f_{ex}\to v}(\omega) = \frac{\mathbb{R}\mathrm{e}(G)^2 + \mathbb{I}\mathrm{m}(G)^2}{2\mathbb{R}\mathrm{e}(G)}. \qquad (12)$$

Then, comparing Eq. (8) and Eq. (12),

$$B_r(\omega) = \frac{\mathbb{R}\mathrm{e}(G)}{\mathbb{R}\mathrm{e}(G)^2 + \mathbb{I}\mathrm{m}(G)^2}. \qquad (13)$$

Equivalently, an impedance-matching-based controller can be derived in a feedforward structure, as shown in Fig. 3. Then, for analytical derivation of the controller, a perfect knowledge of the excitation force is assumed, viz

$$f_{ex}(t) = \hat{f}_{ex}(t), \qquad (14)$$

where $\hat{f}_{ex}(t)$ represents an excitation force estimate. Nevertheless, as considered in a realistic implementation of the proposed controller (described in Section IV), the application case is analysed using an excitation force estimator, i.e. $f_{ex}(t) \approx \hat{f}_{ex}(t)$.

Assuming that the optimal velocity profile can be obtained from Eq. (12), then defining

$$H_{ff}(w) = \frac{\mathbb{R}\mathrm{e}(G) + \jmath\mathbb{I}\mathrm{m}(G)}{2\mathbb{R}\mathrm{e}(G)}, \qquad (15)$$

the mapping from $F_{ex}(\omega)$ to $V(\omega)$, in the FF structure, is equivalent to that presented in Eq. (12).[2] Thus,

$$F_u(\omega) = H_{ff}(\omega)\hat{F}_{ex}(\omega). \qquad (16)$$

Using system identification algorithms [26]–[28], we approximate $H_{ff}(\jmath\omega)$ with a LTI-stable and implementable dynamical system $\tilde{H}_{ff}(s)$, i.e.:

$$\tilde{H}_{ff}(s)\Big|_{s=\jmath\omega} \approx H_{ff}(\omega). \qquad (17)$$

In the identification procedure, the input *a-priori* information is given by the frequency domain data set $H_{ff}(\omega)$, while the

identification output is given by the LTI dynamical system $\tilde{H}_{ff}(s)$. With regard to the identification process, some fundamental aspects are worth highlighting. Firstly, in order to guarantee that a stable LTI system is obtained from the identification, stability must be set as a requirement in the identification algorithm. Secondly, since the identification is defined using frequency-domain data, frequency-domain system identification algorithms, such as moment-matching-based [28] or subspace-based methods [29], are recommended. In particular, we consider moment-matching-based identification algorithms, allowing for a perfect match at specific-user defined frequency values, which can be useful in oscillatory processes, such as the wave energy case.

In order to define the energy maximising controller, as expressed in Eq. (17), some aspects need to be considered:

✓ *Dynamical system:* Since the frequency domain data set employed as input to the identification algorithm does not correspond with a dynamical parametric system, i.e. the data set does not come as an input-output pair from a classical physical system, it is necessary to define an *a-priori* frequency matching bandwidth in which the identification algorithm must be focussed. Then, Eq. (17) holds $\forall s = \jmath\omega, \omega \in BW = [\omega_i, \omega_f] \subset \mathbb{R}^+$. It is important to note that $BW$ should correspond to the frequency band with the largest power density for the excitation force [28].

✓ *Excitation force peak frequencies:* As mentioned in the previous item, the excitation force frequency (spectral) information, mainly its power spectral density (PSD), is a key driver in the definition of the target frequency bandwidth $BW$. The frequency range with the largest PSD for the excitation force, must be considered in the definition of $BW$. In other words, the maximum values of the PSD, including the so-called peak (or typical) frequency, are always contained in $BW$. Note that all the commonly used waves spectral models, such as the JONSWAP spectrum defined in [30], are defined using a typical period, which is intrinsically linked with the peak frequency.

✓ *$\tilde{H}_{ff}(s)$ order:* As is usual in system identification problems, there is a trade-off between the identified system order and the fitting error. Depending on the specific requirements of each case, it may be preferable to reduce the identified system order, losing fitting performance, but achieving a more computationally efficient implementation [31], [32]. In the LiTe-Con case, given the simplicity of the controller structure, the controller order does not represent a challenge, thus a high-order structure, which describes the data with significant fidelity, can be used.

✓ *Transient effects:* An additional frequency domain criterion is related to transient effects. The complete frequency response, outside the matching frequency bandwidth, has a direct impact on the transient response, which can significantly degrade the resulting performance.

### C. Constraint Handling

As extensively described in the literature [1], a common issue in controlled WECs is that the controller often demands excessive device displacement to achieve the theoretical optimal

---

[2]Note that each term in Eq. (15) has an equivalent term in the solution of the quadratic optimisation problem defined in MM/Sp/Ps-based control problems for the unconstrained case. A precise discussion about a MM-based control can be found in [10]. Additionally, please refer to [11] and [22] for detailed discussions about control strategies based on and Sp/Ps methods.

performance. As a result, several constraint handling mechanisms have been proposed in the literature. In the case of [9], the controller uses an EKF to estimate an instantaneous excitation force frequency and amplitude, which are explicitly used to modulate the optimal velocity profile, aiming to keep the device within the specified motion constraints. MPC-like or MM/Sp/Ps strategies, such as [10], or [16], implement physical limitations by constraining the corresponding optimisation problem according to both the device and PTO characteristics. Additionally, traditional latching/declutching methods [33] deal with displacement constraints by absorbing, with the physical structure, the mechanical effort, which can overload the latching/declutching mechanism.

Unlike the aforementioned control approaches, this study proposes a LTI amplitude displacement constraint handling strategy. Two main goals are considered in the constraint handling strategy: (a) preserve the essential zero-phase locking condition between $F_{ex}(\omega)$ and $V(\omega)$ (see Eq. (8)); and (b) restrict the device velocity and displacement using a constant value $k \in [0, 1]$, as follows:

$$0 \leq k|v(t)| \leq |v^{opt}(t)|, \text{ with } k \in [0, 1]. \tag{18}$$

Then, in terms of the performance defined in Eq. (6), the resulting performance is given by:

$$0 \leq -\int_0^T (kv(t))f_u(t)dt. \leq -\int_0^T v(t)f_u(t)dt, \tag{19}$$

which guarantees a non-negative energy absorption for $k \in [0, 1]$. Equation (19) shows a trade-off between the velocity constraint, translated into a displacement constraint, and the resulting performance, i.e. a greater displacement restriction generates a more significant drop in performance. Then, in terms of $\mathbb{Re}(G)$ and $\mathbb{Im}(G)$, using Eq. (12), the force-to-velocity mapping incorporating $k$ is

$$T_{f_{ex} \to v}(\omega) = \frac{k\left(\mathbb{Re}(G)^2 + \mathbb{Im}(G)^2\right)}{2\mathbb{Re}(G)}. \tag{20}$$

Then, the effect of $k$ in $T_{f_{ex} \to v}(\omega)$ can be included in Eq. (15)

$$\bar{H}_{ff}(\omega) = \frac{(2-k)\mathbb{Re}(G) + kj\mathbb{Im}(G)}{2\mathbb{Re}(G)}. \tag{21}$$

Note that, in Eq (21), if $k = 1$, then $\bar{H}_{ff}(\omega)$ matches the expression in Eq. (15). On the other hand, if $k = 0$, then $T_{f_{ex} \to v}(\omega) = 0$.

From Equations (15), (20), and (21), when the constraint handling mechanism is included, using the LTI approximation in Eq. (17), the control force can be expressed as follows:

$$F_u(\omega) = \underbrace{\left[k\tilde{H}_{ff}(\omega) + (1-k)\right]}_{\text{Controller}} F_{ex}(\omega). \tag{22}$$

Eq. (22) is schematically presented, in Fig. 4, where the controller is depicted inside the dotted-blue box.

Note that the constraint handling mechanism, described in Equations (18)–(22), can restrict the velocity and the position between their equilibrium values, which in realistic conditions are both zero, and their constraint limits, while preserving the
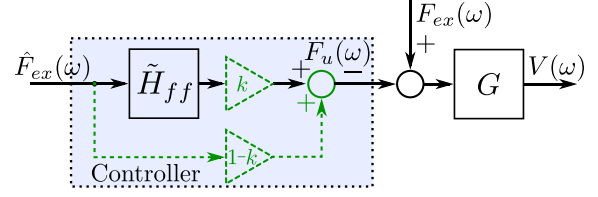


Fig. 4. Final force-to-velocity scheme. The blue box indicates the control structure including the constraint handling mechanism.

zero-phase-locking between the velocity and the wave excitation force.

The determination of $k$ can be performed using: (a) statistical *a-priori* excitation force information, e.g. the maximum value for $f_{ex}(t)$; (b) simulations under polychromatic sea states, for different stochastic realisations (empirically); and (c) adaptive methods reducing (increasing) $k$ when displacement saturations are detected (not detected).

Note that, due to the individual stability of the controller $\tilde{H}_{ff}(s)$, estimator, and the system $G(s)$, the final force-to-velocity stability is guaranteed under the separability principle [34], which states that, given the linear nature of each system involved, the controller and estimator (observer) can be designed separately.

## IV. APPLICATION CASE

This section presents an application of the LiTe-Con control structure introduced in Section III-B. For performance assessment, two existing controller structures are considered for reference: a Sp-based controller, and SaE controller. Unlike the unconstrained case, in which the theoretical maximum performance can be straightforwardly computed, there is not an explicit formulation for the maximum achievable performance in the constrained case. Even though the resulting performance obtained with optimisation-based formulations, e.g. MPC/MM/Sp/Ps-based, is not a theoretical maximum, it can be considered as a reference for maximum achievable constrained performance. So, with the aim of obtaining a performance benchmark, a Sp-based controller is used in this application case for the performance comparison in the constrained case. Additionally, the SaE controller is used in the performance comparison since, as mentioned in Section I, the SaE controller can be considered the closest reference in the WEC control literature to the LiTe-Con controller proposed in Section III of this study.

The application case is based on a spherical heaving point absorber WEC model, shown in Fig. 1, similarly to that in [10]. The radius and mass of the device are 5 m and 33543 Kg, respectively. In this application case, the excitation force, $f_{ex}(t)$, considering regular and irregular waves, is determined from the free-surface elevation, $\eta(t)$, which is based on a spectrum $J_\eta(\omega)$. When irregular waves are considered, $J_\eta(\omega)$ is based on a JONSWAP spectrum [30], which provides a statistical description for partially developed sea waves, and the sea state parameters used are a peak period $T_p \in [5.0, 12.0]$ s, significant wave height $H_s = 2.0$ m, and a steepness parameter $\gamma = 3.3$.
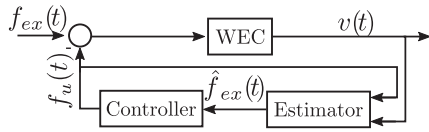
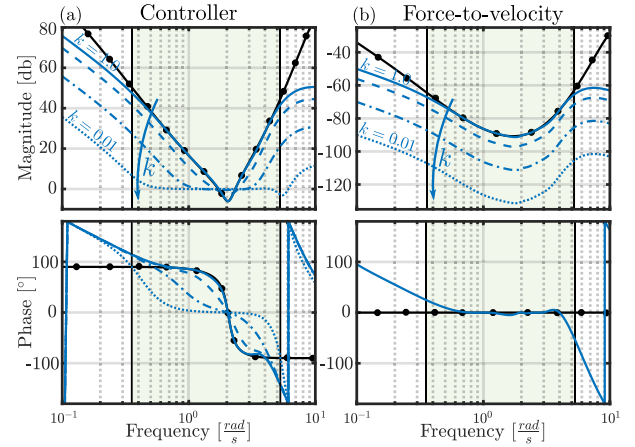Fig. 5.    LiTe-Con controller implementation structure.



Fig. 6.    (a) Controller frequency response. (b) Final force-to-velocity frequency response. With solid black line with black dots the theoretical optimal response is shown, while with a solid blue line the identification result is depicted.

Equivalently, when regular waves are considered, the wave height and period are $H = 2.0$ m and $T \in [5.0, 12.0]$ s, respectively, leading to an even spectrum $J_\eta(\omega)$. Then, the power spectral density of the excitation force is given by the relation $|F_{ex}(\omega)| = |G_e(\omega)||J_\eta(\omega)|$, where $G_e(\omega)$, obtained from NEMOH [24], represents the mapping from $\eta(t)$ to $f_{ex}(t)$. The resulting performance is studied in both the constrained and unconstrained cases. Additionally, in the constrained case, the maximum displacement is set to $X_{\max} = 1.5$ m.

In this application case, the value of the constant $k$, for the constraint handling mechanism described in Equations (18)–(22), is determined using exhaustive simulation-based search, depending on each particular sea state considered.

The performance, measured in terms of the absorbed energy, is shown in absolute terms, as well as relative to the standard deviation of the excitation force $\sigma\{f_{ex}(t)\}$. Thus, increments in performance are isolated from increases in the excitation force power.

As discussed previously in this section, the proposed LiTe-Con controller is compared with the SaE controller and a Sp-based controller. Given the features of each controller, the simulations are performed as follows:

1) *LiTe-Con:* Based on the comprehensive review in [18], a standard Kalman filter (KF) including a harmonic oscillator, is chosen for the estimation of the wave excitation force. In particular the KF with a harmonic oscillator is based on a LTI structure and, as shown in [18], its accuracy and noise handling are worth highlighting. A block diagram of the implementation structure is shown in Fig. 5.

2) *SaE Controller:* This control structure requires an EKF (non-linear) for instantaneous amplitude and frequency estimation. Then, the resulting performance largely depends on the EKF estimation procedure, in addition to the control structure. In this study, perfect knowledge of the instantaneous amplitude and frequency of the excitation force is assumed, to avoid performance degradation related to estimator tuning. Similar to the LiTe-Con case, a standard KF including a harmonic oscillator for excitation force estimation is used. More details about the implementation of this controller can be found in [9]. Additionally, considering the fact that the SaE controller achieves its best performance when the device is excited by waves of a narrow-banded nature [9], and to provided the best scenario for the SaE controller in the performance assessment subsequently presented in this paper, narrow-banded JONSWAP spectrum-based waves are considered in this study.

3) *Sp Controller:* To use the Sp-based controller as a benchmark for the maximum achievable performance in the constrained case, *a-priori* perfect knowledge of the excitation force is assumed. Additionally, a set of truncated Fourier basis functions is used in this study for the implementation of the Sp-based controller. A detailed discussion about the implementation of this family of controllers can be found in [11], [22].

In general, since the accuracy of the excitation force is indeed a potential issue in the final controller performance, some aspects about the estimator shown in Fig. 5, can be mentioned. Different wave excitation force estimation methods have been proposed throughout the literature. A recent review and comparison of recent excitation force estimation methods is available in [18]. As mentioned before, a standard KF, including a harmonic oscillator, is chosen for this application case. In addition, the KF-based estimation approach employed in this study is, as the controller, based on a LTI structure. Note that, though the effect of the accuracy of the excitation force estimation is not directly addressed in the paper, this has been subject of previous studies, such as [5] and [17]. Thus, to strictly focus on the control problem, neither model uncertainty nor measurement noise have been considered in this study, therefore, the obtained estimation accuracy is close to 100%. Then, in the application case, the effect of the estimator on the resulting control performance is negligible.

### A. Controller Identification and Optimal Force-to-Velocity Mapping

The controller identification results, as explained in Section III, are shown in Fig. 6. The identification is performed using a MM-based identification approach to ensure perfect matching at precise frequencies, which can be related to a particular sea state [28]. In this study, the fitting band is set to $BW = [0.35, 5.10]\ \frac{\text{rad}}{\text{s}}$, which is highlighted with a shaded green area in Fig. 6. According to MM-based identification theory [16], the controller order is twice the number of matching points. In this study, 6 matching points are considered, which are the system resonance frequency $w_r = 2.035\ \frac{\text{rad}}{\text{s}}$, $\omega = 4$ $\frac{\text{rad}}{\text{s}}$, which is, according to the target $BW$, to ensure certain
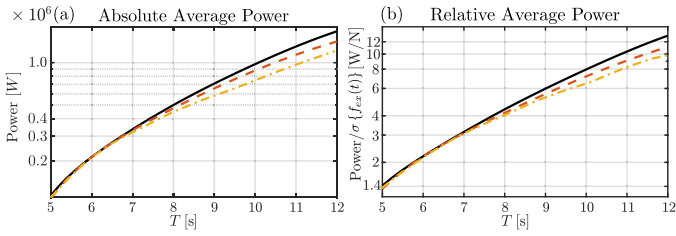
Fig. 7. Generated power for the unconstrained case with regular waves. The results obtained using the LiTe-Con and the SaE controllers are shown using dashed orange and dash-dotted yellow lines, respectively. The theoretical maximum is depicted using a solid black line.



Fig. 9. Generated power for the constrained case with irregular waves. The results obtained using the Sp-based control, the LiTe-Con controller, and the SaE controller are shown using solid blue, dashed orange, and dash-dotted yellow lines, respectively.
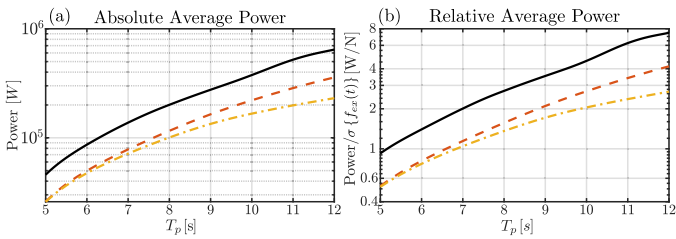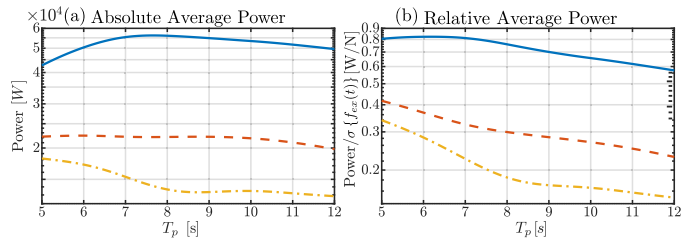


Fig. 8. Generated power for the unconstrained case with irregular waves. The results obtained using the LiTe-Con and the SaE controllers are shown using dashed orange, and dash-dotted yellow lines, respectively. The theoretical maximum is depicted using a solid black line.

bandwidth in the identification optimisation, and the remaining 4 points, $\omega = \{0.79,\ 0.97,\ 2.50,\ 2.80\}\ \frac{\text{rad}}{\text{s}}$, are defined optimally in order to improve the fit between $H_{ff}(\omega)$ and $\tilde{H}_{ff}(\omega)$ within $BW$ [16]. Consequently, the obtained controller order is 12. In Fig. 6(a) (the left-hand side column), the controller identification result is shown, while in Fig. 6(b) (the right-hand side column), the final force-to-velocity mapping is shown. The upper and lower rows are related to the magnitude and phase of the frequency response, respectively. The optimal theoretical frequency responses $H_{ff}(\omega)$ and $T_{f_{ex} \to v}^{opt}(\omega)$ (see Equations (12) and (17)), are shown with a solid black line with black dots in Figs. 6(a) and 6(b), respectively. The frequency response of the obtained controller, $\tilde{H}_{ff}(\omega)$, and the obtained force-to-velocity mapping, when $\tilde{H}_{ff}(\omega)$ is used, is shown with a solid blue line in Figs. 6(a) and 6(b), respectively. Additionally, in Fig. 6, when the constraint handling mechanism is considered, the cases when $k \in \{1,\ 0.5,\ 0.1,\ 0.01\}$ are shown in solid, dashed, dash-dotted, and dotted blue lines, respectively.

*B. Performance Results*

In Fig. 7, the obtained performance, measured in terms of average generated power, is shown for the unconstrained case, under monochromatic excitation.

Analogously to Fig. 7, Figs. 8 and 9 present performance results for polychromatic waves, under both unconstrained and constrained (displacement) cases, respectively. For Figs. 7, 8, and 9, the absolute generated power, and the generated power relative to the excitation force standard deviation $\sigma\{f_{ex}(t)\}$, are shown in columns (a) and (b), respectively. In Figs. 7, 8, and 9, the results obtained with the LiTe-Con and

SaE controllers are depicted with dashed orange and dash-dotted yellow lines, respectively. In Figs. 7 and 8, the maximum theoretical achievable performance is depicted with a solid black line. For the constrained case, shown in Fig. 9, the maximum achievable performance, obtained with the Sp-based controller, is depicted with a solid blue line. From the results shown in Figs. 7, 8, and 9, there are some aspects which are worth highlighting. Firstly, note that the unconstrained case, using regular waves, depicted in Fig. 7, explicitly shows the behaviour of the system in steady-state, which matches the well-known result for impedance-matching-based controllers shown in Eq. (9).[3] In addition, the LiTe-Con controller performace in Fig. 7 is equivalent to the theoretical maximum, depicted in Fig. 7 using a solid black line. Secondly, the different performance levels achieved by the LiTe-Con controller, in Figs. 7 and 8, are intrinsically related to the power spectral density (PSD) of each excitation force, regular and irregular, in Figs. 7 and 8, respectively. Note that, in the case of Fig. 7, i.e. using regular waves, the PSD of the excitation force is entirely contained in an infinitely narrow frequency band, while in the case of Fig. 8, i.e. using irregular waves, the PSD is distributed over a broader frequency range. On the other hand, the result shown in Fig. 8, also in the unconstrained case but using irregular waves, shows that the performance of the LiTe-Con controller is lower than the theoretical maximum. This performance degradation observed between the LiTe-Con controller and the theoretical maximum, in Fig. 8, which is not observed in the unconstrained case using regular waves shown in Fig. 7, is generated as a consequence of the *"continuous"* transient response generated by the use of irregular waves. Note that in the unconstrained case using regular waves, in Fig. 7, the results, as mentioned before, describe the steady-state response. In addition, in the results shown in Fig. 9, the constraints are handled by the LiTe-Con controller with a general gain decrease, significantly affecting performance, while in the case of the spectral controller the constraints are handled in an optimal way by means of optimisation routines. Finally, to reduce the performance degradation in the LiTe-Con case observed between Fig. 7 (regular waves) and Fig. 8 (irregular waves), $BW$ should be extended to include higher frequencies;

---

[3]Note that, this paper does not address the study of regular waves in the constrained case since the most realistic scenario, in terms of real operation conditions, is given by the use of irregular waves, which have been studied in the manuscript as shown in Figs. 8 and 9.
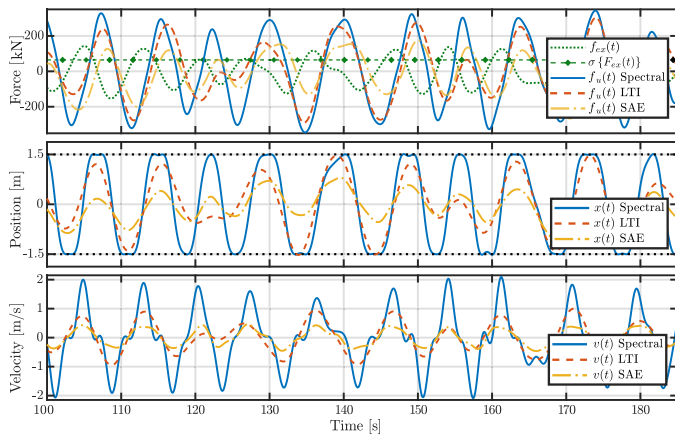
Fig. 10. Time response for the constrained case using irregular waves with peak period $T_p = 8.5$ s and significant wave height $H_s = 2$ m. The maximum displacement is set to $X_{\max} = 1.5$ m.

however, this could reduce the fit in the bandwidth in which most of the PSD of the excitation force is contained. On the other hand, this effect can be neglected when regular waves are considered, as shown in Fig. 7.

### C. Time Domain Performance

In Fig. 10, the results obtained with each control strategy studied are shown. The results shown in Fig. 10 are obtained using an irregular wave, with peak period $T_p = 8.5$ s and significant wave height $H_s = 2.0$ m, while the maximum displacement is set to $X_{\max} = 1.5$ m. The excitation force $f_{ex}(t)$ (the excitation force standard deviation $\sigma\{f_{ex}(t)\}$), measured in kilonewton [kN], is depicted with the dotted (dashed) green line (green line with square markers) in the top plot of Fig. 10. The control force, position, and velocity are shown in the top, middle, and bottom plots of Fig. 10, respectively. Additionally, the results obtained with the Sp-based, LiTe-Con, and SaE controllers are shown using solid blue, dash-dotted yellow, and dashed orange lines, in Fig. 10, respectively. Some comments can be made from the analysis of the time response, shown in Fig. 10. Firstly, the excitation force (top plot) preserves zero-phase locking with respect to the velocity obtained using the LiTe-Con controller (bottom plot), which is, as noted in Section III, a key driver in power production with WECs. Secondly, from the middle plot in Fig. 10, the LiTe-Con constraint handling mechanism keeps the device within the specified motion constraints. Additionally, the LiTe-Con controller obtains larger displacement (and velocity) than the SaE controller, which is translated into more power production. Finally, from the top plot in Fig. 10, it can be seen that the control force, generated by the LiTe-Con controller, is approximately shifted $90°$ with respect to the excitation force, coinciding with the well-known optimal condition [3].

## V. Conclusion

This study proposes a novel framework for the design of a LTI energy maximising control, called LiTe-Con, which, even though is initially inspired by WEC systems, can be adapted and applied to a number of different energy maximising control

problems. For example, in a solar power maximisation problem, the device velocity and controller force, considered in this study, would be replaced by current and voltage, respectively. The design procedure is based on the impedance-matching principle of optimality, providing a broadband solution for energy maximising control problems. It is important to note that the broadband nature of the presented control structure can efficiently extract energy under both monochromatic and polychromatic wave processes. Additionally, the design procedure requires a trade-off between the target bandwidth, in which the energy maximising control is focused, and the identification accuracy.

When displacement restrictions are considered, a constraint handling mechanism, which guarantees zero-phase locking between the excitation force and the system velocity, is provided. Furthermore, the device displacement is strictly contained between zero and a maximum displacement, given by the condition of optimality, while a constant parameter $k$ varies in $[0, 1]$.

From a general perspective, the proposed energy maximising control structure constitutes an alternative LTI controller that, while being suboptimal in the constrained case, is simple and effective at the same time, which makes it suitable for implementation in realistic applications. It is important to note that the controller simplicity also implies that: (1) the controller can be designed and implemented by non-specialised technicians [37], requiring only a basic understanding of frequency response; (2) the controller can be implemented in almost any physical hardware platform, such as commercial low cost microcontrollers; and (3) implementation and programming efforts, and numerical errors can be significantly reduced. Summarising, as demonstrated in this paper, the proposed LiTe-Con controller offers a parsimonious balance between simplicity and energy-maximising performance, suggesting it as a strong candidate for realistic and commercial WEC applications. Additionally, from the performance assessment performed in Section IV, it can be seen that the obtained performance of the LiTe-Con controller, is greater than that obtained with the SaE controller, for both the unconstrained and constrained cases. Additionally, even though the power production obtained with the LiTe-Con is lower than the maximum achievable with optimisation-based controllers, the design and implementation of the LiTe-Con controller is considerably simpler.

## References

[1] J. V. Ringwood, G. Bacelli, and F. Fusco, "Energy-maximizing control of wave-energy converters: The development of control system technology to optimize their operation," *IEEE Control Syst. Mag.*, vol. 34, no. 5, pp. 30–55, Oct. 2014.

[2] U. A. Korde and J. V. Ringwood, *Hydrodynamic Control of Wave Energy Devices.* Cambridge, U.K.: Cambridge Univ. Press, 2016.

[3] J. Falnes, *Ocean Waves and Oscillating Systems: Linear Interactions Including Wave-Energy Extraction.* Cambridge, U.K.: Cambridge Univ. Press, 2002.

[4] J. Falnes, "A review of wave-energy extraction," *Marine Struct.*, vol. 20, no. 4, pp. 185–201, 2007.

[5] J. V. Ringwood, A. Mérigaud, N. Faedo, and F. Fusco, "An analytical and numerical sensitivity and robustness analysis of wave energy control systems," *IEEE Trans. Control Syst. Technol.*, to be published, Apr. 2019.

[6] R. H. Hansen, "Design and control of the power take-off system for a wave energy converter with multiple absorbers," Ph.D. dissertation, Dept. Energy Technol., Aalborg University, Aalborg, Denmark, 2013.

[7] A. Clément and A. Babarit, "Discrete control of resonant wave energy devices," *Philosophical Trans. Roy. Soc. A*, vol. 370, no. 1959, pp. 288–314, 2012.

[8] J. Hals, J. Falnes, and T. Moan, "Constrained optimal control of a heaving buoy wave-energy converter," *J. Offshore Mech. Arctic Eng.*, vol. 133, no. 1, 2011, Art. no. 011401.

[9] F. Fusco and J. V. Ringwood, "A simple and effective real-time controller for wave energy converters," *IEEE Trans. Sustain. Energy*, vol. 4, no. 1, pp. 21–30, Jan. 2013.

[10] N. Faedo, G. Scarciotti, A. Astolfi, and J. V. Ringwood, "Energy-maximising control of wave energy converters using a moment-domain representation," *Control Eng. Pract.*, vol. 81, pp. 85–96, 2018.

[11] D. Garcia-Violini and J. V. Ringwood, "Energy maximising robust control for spectral and pseudospectral methods with application to wave energy systems," *Int. J. Control*, 2019.

[12] M. Penalba, J. Davidson, C. Windt, and J. V. Ringwood, "A high-fidelity wave-to-wire simulation platform for wave energy converters: Coupled numerical wave tank and power take-off models," *Appl. Energy*, vol. 226, pp. 655–669, 2018.

[13] J. A. Cretel, G. Lightbody, G. P. Thomas, and A. W. Lewis, "Maximisation of energy capture by a wave-energy point absorber using model predictive control," *IFAC Proc. Volumes*, vol. 44, no. 1, pp. 3714–3721, 2011.

[14] A. F. O. Falcão, P. A. Justino, J. C. Henriques, and J. M. André, "Reactive versus latching phase control of a two-body heaving wave energy converter," in *Proc. IEEE Euro. Control Conf.*, 2009, pp. 3731–3736.

[15] A. Babarit and A. H. Clément, "Optimal latching control of a wave energy device in regular and irregular waves," *Appl. Ocean Res.*, vol. 28, no. 2, pp. 77–91, 2006.

[16] N. Faedo, S. Olaya, and J. V. Ringwood, "Optimal control, MPC and MPC-like algorithms for wave energy systems: An overview," *IFAC. Syst. Control*, vol. 1, pp. 37–56, 2017.

[17] F. Fusco and J. V. Ringwood, "A model for the sensitivity of non-causal control of wave energy converters to wave excitation force prediction errors," in *Proc. 9th Eur. Wave Tidal Energy Conf.*, 2011[CD-ROM].

[18] Y. Peña-Sanchez, C. Windt, D. Josh, and J. V. Ringwood, "A critical comparison of excitation force estimators for wave energy devices," *IEEE Trans. Control Syst. Technol.*, to be published, Sep. 2019.

[19] T. Sun and S. R. Nielsen, "Stochastic control of wave energy converters for optimal power absorption with constrained control force," *Appl. Ocean Res.*, vol. 87, pp. 130–141, 2019.

[20] M. Richter, M. E. Magaña, O. Sawodny, and T. K. Brekken, "Power optimisation of a point absorber wave energy converter by means of linear model predictive control," *IET Renew. Power Gener.*, vol. 8, no. 2, pp. 203–215, 2013.

[21] G. Li and M. R. Belmont, "Model predictive control of sea wave energy converters–part ii: The case of an array of devices," *Renew. Energy*, vol. 68, pp. 540–549, 2014.

[22] G. Bacelli and J. V. Ringwood, "Numerical optimal control of wave energy converters," *IEEE Trans. Sustain. Energy*, vol. 6, no. 2, pp. 294–302, Apr. 2015.

[23] Wamit Inc, "WAMIT user manual," 2019. [Online.] Available: http://tinyw.in/7u4T, Accessed: Aug. 1, 2019.

[24] LHEEA, NEMOH-Presentation, "Laboratoire de Recherche en Hydrodynamique Énergetique et Environnement Atmospherique," 2017. [Online.] Available: https://goo.gl/yX8nFu, Accessed: Aug. 1, 2019.

[25] J. Hals, J. Falnes, and T. Moan, "A comparison of selected strategies for adaptive control of wave energy converters," *J. Offshore Mech. Arctic Eng.*, vol. 133, no. 3, pp. 031 101–031 113, 2011.

[26] P. V. Overschee and B. De Moor, *Subspace Identification for Linear Systems - Theory Implication Applications*. Berlin, Germany: Springer, 1996.

[27] L. Ljung, *System Identification - Theory for the User*. Englewood Cliffs, NJ, USA: Prentice-Hall, 1999.

[28] N. Faedo, Y. Peña-Sanchez, and J. V. Ringwood, "Finite-order hydrodynamic model determination for wave energy applications using moment-matching," *Ocean Eng.*, vol. 163, pp. 251–263, 2018.

[29] P. Van Overschee and B. De Moor, "N4sid: Subspace algorithms for the identification of combined deterministic-stochastic systems," *Automatica*, vol. 30, no. 1, pp. 75–93, 1994.

[30] K. Hasselmann, "Measurements of wind wave growth and swell decay during the Joint North Sea Wave Project (JONSWAP)," *Deutches Hydrographisches Institut*, vol. 8, 1973, Art. no. 95.

[31] R. S. Sánchez-Peña and F. D. Bianchi, "Model selection: From LTI to switched-LPV," in *Proc. IEEE Amer. Control Conf.*, 2012, pp. 1561–1566.

[32] M. Gevers, "Identification for control: From the early achievements to the revival of experiment design," *Eur. J. Control*, vol. 11, no. 4/5, pp. 335–352, 2005.

[33] A. Babarit, M. Guglielmi, and A. H. Clément, "Declutching control of a wave energy converter," *Ocean Eng.*, vol. 36, no. 12, pp. 1015–1024, 2009.

[34] G. C. Goodwin *et al.*, *Control System Design*, vol. 240. Englewood Cliffs, NJ, USA: Prentice-Hall, 2001.

[35] R. S. Sánchez-Peña, J. Q. Casín, and V. P. Cayuela, *Identification and Control The Gap between Theory and Practice*. Berlin, Germany: Springer, 2007.

**Demián García-Violini** received the B.S. degree in automation and control engineering from the National University of Quilmes, Buenos Aires, Argentina, in 2010, and the Doctoral degree in engineering from the Buenos Aires Institute of Technology, Buenos Aires, Argentina, in 2015. He is currently a Postdoctoral Researcher with the Centre of Ocean Energy Research, National University of Ireland, Maynooth, Ireland.

**Yerai Peña-Sanchez** received the Diploma degree in renewable energies engineering from the University of the Basque Country, Leioa, Spain, in 2016. He has been working toward the Ph.D. degree with the Centre for Ocean Energy Research, Maynooth University, Maynooth, Ireland, since 2016. He is working on estimation and forecasting of wave excitation force.

**Nicolás Faedo** received the degree in automation and control engineering from the National University of Quilmes, Buenos Aires, Argentina, in 2015. He has been working toward the Ph.D. degree in nonlinear control of wave energy devices with the Centre for Ocean Energy Research, since 2017. He worked for a year, holding an undergraduate scholarship, in model identification and optimization of cold rolling processes.

**John V. Ringwood** (Senior Member, IEEE) received the Diploma degree in electrical engineering from the Dublin Institute of Technology, Dublin, Ireland, in 1981, and the Ph.D. degree in control systems from Strathclyde University, Glasgow, Scotland, in 1985. He is currently a Professor of electronic engineering with the National University of Ireland, Maynooth, Ireland, and an Associate Dean for engineering with the Faculty of Science and Engineering. His research interests include time series modeling, wave energy, control of plasma processes, and biomedical engineering.